World J Urol (2004) 22: 382–391
DOI 10.1007/s00345-004-0425-9

TOPIC PAPER

E. Andipa · K. Liberopoulos · C. Asvestis

Magnetic resonance imaging and ultrasound evaluation of penile and testicular masses

Received: 28 April 2004 / Accepted: 28 April 2004 / Published online: 6 August 2004

Abstract The purpose of this study is to present the role of ultrasonography and MRI in the investigation of testicular and penile masses, as well as to review the literature. This article is based on our experience with 230 patients who presented with acute or subacute scrotal pain or painless enlargement of the scrotum or penis. Gray scale and color Doppler ultrasonography (CDU) were applied in all cases. In 73 cases, the final diagnosis was established by surgery and in 157 cases by follow-up. MRI was performed in 48 cases. Ultrasonography was the initial imaging modality in all cases. It provided detailed anatomic information with high sensitivity and accuracy in cases of torsion, inflammation, varicocele and trauma. In cases of tumor, US showed the presence of the mass in all cases, while it additionally revealed certain characteristic features of tissue constitution and blood supply. In most cases, differentiation between various types of tumors or differentiation between malignant and benign lesions was impossible. MRI, besides the detailed anatomic imaging, also provided a certain degree of tissue specificity. MRI could help in the detection and staging of penile cancer and in the evaluation of testicular and scrotal masses, especially when a diagnostic dilemma occurred on ultrasonographic examination. Ultrasonography, combining gray scale and color techniques, is irreplaceable in the diagnostic work-up of scrotal and penile masses, while MRI can serve as a problem solving diagnostic modality.

Keywords Ultrasound · MRI · Testicular neoplasms · Penile neoplasms · Orcheoepididymitis

E. Andipa · K. Liberopoulos
Department of Radiologic Imaging,
Athens General Hospital "G. Gennimatas",
Athens, Greece

C. Asvestis (✉)
Athenian Group for the Study of Andrological Disease,
4 Maragou, Glyfada 16675, Attica, Greece
E-mail: asvesmed@otenet.gr
Tel.: +30-210-8948213
Fax: +30-210-8948213

The clinical evaluation of the testicular and penile pathology can be difficult and inconclusive. In the majority of cases, the clinical manifestation, including pain, edema and enlargement, as well as the findings on palpation and laboratory tests, can lead to an accurate diagnosis. On the other hand, there are cases in which the diagnosis is possible only with the aid of imaging techniques, such as ultrasound (US), color Doppler ultrasonography (CDU) and magnetic resonance imaging (MRI). Such problematic cases can involve testicular tumors, subacute chronic orcheoepididymitis, lymphomas, testicular infarction, and late diagnosed testicular torsion. In cases of testicular trauma, the integrity of the tunica albuginea has to be confirmed in order to avoid surgical exploration. Penile neoplastic pathology is another area where precise information about the location, the extent and the involvement of the disease will enable the surgeon to perform the correct procedure.

Nowadays, high resolution ultrasonography is considered as an extension and supplement to clinical evaluation, being the imaging modality of choice for the evaluation of testicular, scrotal and penile diseases. Advances in technology, with the introduction of high frequency probes, have significantly improved the diagnostic confidence of the method, providing information on the normal anatomy, the morphological features, as well as relevant data on the vascular supply of the lesions examined. Additionally, ultrasound examination can be performed with minimal patient discomfort, at low cost and without ionizing radiation.

Nevertheless, there are cases in which both clinical examination and US fail to establish the correct diagnosis. The use of MRI has been suggested in previous studies as an alternative imaging method for a variety of diseases involving the testis and penis when US is

inconclusive. MRI provides detailed high resolution images of both testes and penis without the use of ionizing radiation. The multiplanar capabilities of the technique, combined with the high contrast resolution, can add valuable information towards the diagnosis.

Here, we review the normal US and MRI anatomy of the scrotum and penis, discuss the technical features of these imaging modalities and provide the US and MRI findings for various pathological entities, such as inflammation, torsion, trauma and neoplasms of the testis, as well as, the features of penile tumors and Peyronie's disease.

Anatomy

In adults, normal testes are paired oval structures that measure 4–5 cm in the craniocaudal axis and 2–3 cm in the anteroposterior axis. Each testis is composed from 200–300 pyramidal lobules, each one of which contains 400–600 seminiferous tubules. The testis is surrounded by the tunica albuginea, which is composed by fibrous tissue and invaginates into the posterior surface of the gland, forming the mediastinum testis. Septa extend from the mediastinum and divide the gland into pyramidal lobules. In US, the testes appear as oval smooth structures with homogeneous echogenicity. The mediastinum appears as an echogenic band, and the rete testis can be identified in 18% of cases as a hyperechoic area adjacent to the mediastinum. A thin echogenic line around the testis represents the tunica albuginea. On MRI, the normal testis has a high signal intensity on T2W images, slightly lower than that of water (Fig. 1), while on T1W images it appears with intermediate signal intensity. T2W sequences are sensitive in revealing pathologic conditions of the testis, while T1W sequences can help in tissue characterization, such as in the demonstration of fat, hemorrhage and proteinaceous fluid. The tunica albuginea measures about 1 mm in thickness and is of low signal intensity on both T1W and T2W images because of its fibrous nature. The fibrous septa within the testis are depicted as low signal intensity linear structures on T2W images.

The epididymis is attached to the posterior surface of the testis. The superior portion of the epididymis forms the head, the middle portion the body while the inferior forms the tail. The seminiferous tubules converge to larger ducts, called the tubule recti, which drain to the rete testis at the testicular hilum. The rete testis converges to 15–20 efferent ductules that penetrate the mediastinum portion of the tunica albuginea to form the head of the epididymis. The efferent tubules converge to a single convoluted tubule, which runs along the body and the tail, exiting the epididymis as the vas deferens. In US, the epididymal head is usually of the same echogenicity as the testis. It may be difficult to recognize the small body of the epididymis when not enlarged. The tail is smaller than the head and appears as a curved structure at the inferior pole of the testis. The epididymis is of intermediate signal intensity on T1W images and is relatively isointense to the testis, while it is of intermediate intensity on T2W images, lower than that of the testis. The vas deferens are depicted on T2W sequences as tubular formations, with a dark wall and slightly bright lumen.

The testicular, deferential and cremasteric arteries supply blood to the scrotum. Testicular arteries arise from the abdominal aorta beneath the renal arteries, cross the ureters and the external iliac arteries and enter the spermatic cord at the inguinal ring. They represent the main vascular supply to the scrotum. Testicular arteries branch at the upper pole of the testis, penetrate the tunica albuginea and form the tunica vasculosa. Some branches form the capsular arteries, while others, arising from the capsular arteries, flow to the mediastinum where they form the recurrent rami that carry blood into the testis parenchyma [19, 23, 24] (Fig. 2).The deferential artery, originating from the internal iliac artery, and the cremasteric artery, originating from the inferior epigastric artery, anastomose with the testicular arteries and supply the epididymis, vas deferens and

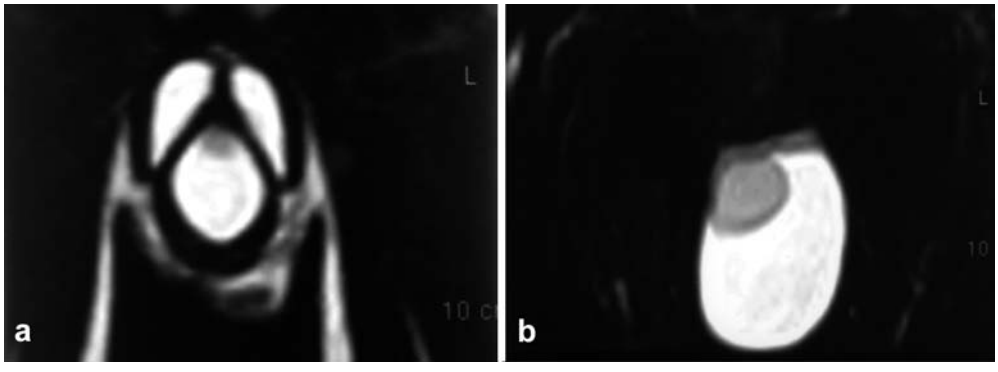

Fig. 1 Normal anatomy. **a** Coronal T2W penile image: the corpus spongiosum and the two corpora cavernosum demonstrate high signal intensity. The tunica albuginea surrounding the three corpora is depicted with low signal intensity. The urethra is detected as a low signal intensity lesion within the corpus spongiosum. **b** Coronal T2W image of the testis: the testis has high signal intensity, but lower than that of water. This becomes obvious by comparing the signal intensity of this normal testis, with the adjacent hydrocele. Tunica albuginea is clearly demonstrated with low signal intensity surrounding the testis

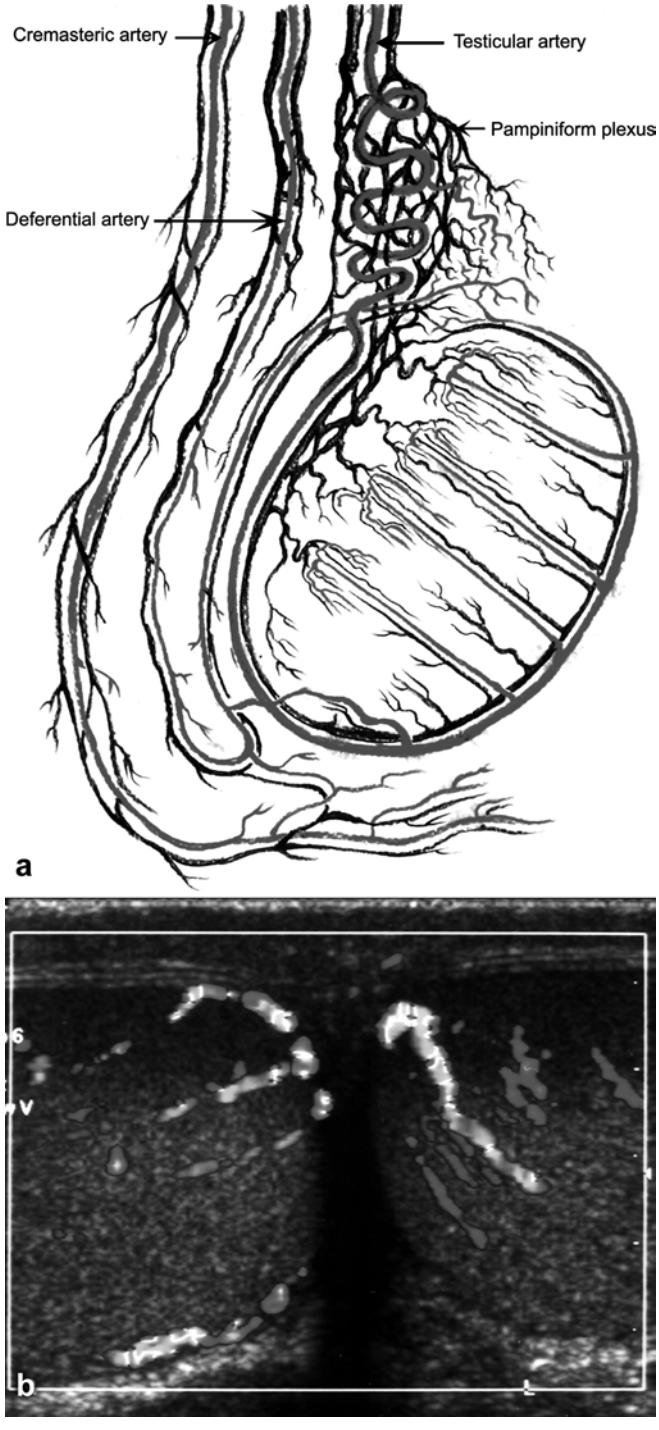

Fig. 2 **a** Schematic demonstration of the normal vascularity of the testis. **b** Normal vessels of the testis. Color Doppler ultrasonography easily depicts the capsular arteries at the periphery of the testis and the centripetal branches coursing to the mediastinum testis

peritesticular tissue with blood. Veins correspond to the arteries. The pampiniform plexus is formed around the epididymis and continues as the testicular vein through the inguinal ring. The right testicular vein empties into the inferior vena cava and the left into the left renal vein [19]. Spectral Doppler analysis reveals a low resistance type of spectrum for the testicular artery and a high resistance type for the deferential and cremasteric arteries [24, 35]. The vascular structures on MRI are shown with low or intermediate signal intensity on T1W or T2W images. The scrotal wall, which is formed by the dartos muscle and fascias, is usually depicted with low signal intensity on T2W images.

The penis is composed by three cylindrical bodies of endothelial trabecular tissue, each of which is surrounded by a tunica albuginea. There are two corpora cavernosa situated dorsally and a corpus spongiosum situated ventrally, in the midline, surrounding the urethra. On US, the corpora cavernosa are relatively hypoechoic in comparison with the corpus spongiosum, which is relatively hyperechoic. The cavernosal arteries are easily found at the base of the penis and the tunica albuginea is depicted as an echogenic line surrounding the corpora. The arterial supply is from the internal pudenal artery, originating from the internal iliac artery and dividing into the dorsal penile, cavernosal and bulbar arteries [24].

On MRI, the cavernosal and spongiosum bodies have an intermediate signal intensity on T1W sequences. On T2W images they appear with increased signal intensity of varying degree, depending on the blood flow at the time. The urethra is easily identified as a low signal intensity structure within the homogeneous high signal intensity of the corpora spongiosum (Fig. 1).

Materials and methods

Our findings are based on the evaluation of 230 patients, 15–45 years old, who presented with acute of subacute scrotum or painless testicular enlargement. We also examined various penile conditions, such as tumors and Peyronie's disease.

Gray scale and CDU were performed in all cases, in 48 of which an MRI study was additionally performed. The results of each imaging modality were compared with the final diagnosis, which was established by the pathologist on a surgical specimen in 73 cases, and with a clinical and imaging follow-up in the remaining 157.

For the ultrasound examination, we used an ATL 5000 HDI unit with a high resolution linear transducer of 5–12 MHz. The patient lay in a supine position with a pad beneath the scrotum and gray scale, color and power Doppler images were obtained in each case. Color velocities were set at ± 4.4 cm/sec and color gain was up to 84%. The power Doppler technique was applied for the detection of lower velocities because of the increased sensitivity of the method to low flow and its independence from Doppler angle correction and aliasing [41]. The testes were examined along the transverse and long axis and the size, echogenicity and vascular supply of each testis, epididymis and spermatic cord were compared to the contralateral side, as well as to the normal anatomy as described in the literature. A convex transducer (2–5 MHz) was used for the evaluation of deep lying lesions, such as, for example, giant hydroceles, hematomas and

hernias. The penis was examined in a dorsiflexed position with the patient supine and identification of the corpora cavernosa, the corpus spongiosum, the surrounding tunica albuginea, as well as the cavernosal arteries was performed with a 5–12 MHz transducer.

All MRI studies were performed using a 1.5 T superconducting magnet. The patients are placed in a supine, feet first position. A circular or rectangular surface coil was used in order to obtain high resolution imaging. Surface coils offer an increased signal-to-noise ratio, thus allowing thin section imaging and small field views. The scrotum was supported by a towel placed between the thighs to avoid motion artifacts, as well as to prevent overlap of the testes. The examination protocol consisted of: (1) axial and coronal T2W turbo spin-echo sequences using a 3 mm slice thickness, FOV of 160 mm, TR 4,000–6,000 ms, TE 120 ms, 4NSA and 192×256 matrix, (2) axial and coronal T1W spin-echo sequences, using a 3 mm slice thickness, FOV 160, TR 600 ms, TE 120 ms, before and after IV injection of gadolinium, (3) a sagittal T2W TSE sequence was obtained when additional information on the epididymis was needed, and (4) additional sequences were obtained using the body coil in order to evaluate inguinal region, upper pelvis and lower abdomen.

The phallus was examined in a dorsiflexed position, which allows visualization of the long axis, as well as the acquisition of symmetrical images of the penis in the coronal plane. The phallus was stabilized with a restraining belt to prevent motion artifacts. The examination protocol included: (1) axial, coronal and sagittal T2W TSE sequences, using 3 mm slice thickness, FOV 180, TR 4,000–6,000 ms, TE 120 ms, 4NSA, and (2) axial and coronal T1W SE sequences before and after IV injection of gadolinium using a slice thickness 3 mm, FOV 180, TR 600 ms, TE 12 ms and 2NSA.

Results

Our findings are summarized in Table 1 where gray scale and color Doppler findings are correlated with the final diagnosis for all patients.

In 95/97 patients with epididymo-orchitis, CDU was able to establish the final diagnosis. Gray scale US was correct in 80/97 cases. Thus CDU proved much more sensitive than gray scale ultrasonography in establishing the correct diagnosis.

Bilateral epididymo-orchitis was found in seven patients, and epididymal or testis abscesses in three cases (Fig 3). In 15 patients, the spermatic cord was swollen, tortuous, with a hypoechoic appearance and increased blood flow as a result of inflammation. Subcutaneous gas within the scrotal wall was found in all three cases, with Fournier gangrene making the diagnosis obvious. In 31 surgically confirmed cases of torsion, gray scale correctly diagnosed the disease in ten cases and CDU in 29 cases. Two patients with incomplete torsion were missed by US. For trauma, gray scale ultrasonography established the diagnosis in 87.5% and CDU in 95.8% of cases. In all cases, blood flow was detected in the spermatic cord. In four patients, rupture of the testis and hematoma were correctly depicted by US, while in one case US was not able to reveal a rupture of the tunica albuginea which was surgically demonstrated. The depiction of venous flow in the scrotum and spectral Doppler analysis can diagnose the presence of varicocele in 100% of cases. Gray scale ultrasonography indicated the diagnosis of the disease in three cases based on the distention of venous plexuses with the depiction of veins >2 mm. In cases of neoplasms, the depicted blood flow was not specific for the determination of histological type, while gray scale ultrasonography was sufficient for the demonstration of the mass. Gray scale ultrasonography can easily depict the presence of hydrocele in 100% of cases. In the case of adrenal rests, clinical and laboratory findings, along with ultrasonographic appearance, strongly indicated the disease, which was finally diagnosed by FNA. In all cases with Peyronie's disease, calcified plaques were easily depicted by gray scale ultrasonography, usually at the site of a palpable mass, making the diagnosis obvious. Cavernosal arteries were depicted in all cases.

False negative results were found in 58 patients with gray scale ultrasonography (25.2%) and in nine patients with CDU (3.9%).

Table 1 Results of ultrasound examination of the scrotum

Final diagnosis	Grey scale	Diagnostic accuracy	Color Doppler	Diagnostic accuracy	Total
Epididymo-orchitis	80	82.5%	95	97.9%	97
Fournier gangrene	3	100%	3	100%	3
Neoplasms	18	81.8%	18	81.8%	22
Tumor like conditions	6	100%	6	100%	6
Cysts adrenal rests	1		1	100%	1
Trauma	21	87.5%	23	95.8%	24
Torsion	10	32.2%	29	93.5%	31
Hydrocele	13	100%	13	100%	13
Varicocele	3	30%	10	100%	10
Inguinal hernia	3	100%	3	100%	3
	Penis				
Peyronie's disease	12	100%	12	100%	12
Neoplasms	6	75%	6	75%	8

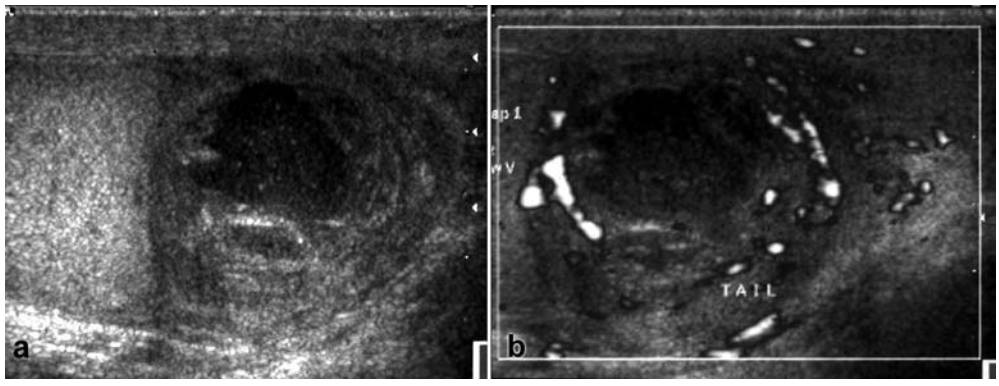

Fig. 3 **a** Epididymal abscess. Grey scale ultrasonography shows an enlarged and inhomogeneous epididymal tail, with a round, hypoechoic focal lesion with irregular walls within. **b** Power Doppler technique depicting the characteristic ring-like peripheral vascularity of the abscess cavity

MRI was performed in four cases of orcheoepididymitis, 17 cases with primary testicular tumors, two cases with testicular cysts, one case of adrenal rest, three cases of torsion, four cases with testicular trauma, four cases of hydrocele, two cases of inguinal hernias, four cases with Peyronie's disease, and seven cases with penile neoplasms.

In terms of testicular and penile tumors, MRI based on T2W images was able to detect the tumors in all 23 cases. A distinction between solid benign and malignant tumors was impossible with MRI. In our series, benign lesions of the penis (fibroma, neuroma, adrenal rests) present with identical MRI characteristics to those of malignant tumors. MRI correctly diagnosed the invasion of the tunica albuginea by tumor in four cases, as this was demonstrated in surgery. This method easily depicted the presence of hydrocele and hernia. In cases of testicular trauma, MRI was able to reveal the interruption of tunica albuginea, which was missed by US. Increased contrast enhancement in the epididymis and spermatic cord was apparent in inflammation, while in cases of torsion enhancement of the spermatic cord could not be detected.

Discussion

Epididymo-orchitis is one of the most common clinical problems. Clinical manifestations vary and the patient may be asymptomatic or report some mild symptoms, while in severe cases fever, abscesses or gangrene may complicate the disease [26, 28]. In young adults, it is usually caused by sexually transmitted organisms such as *Chlamydia trachomatis* and *Neisseria gonorrhoeae*. In patients older than 35 years, *Escherichia coli* and *Proteus mirabilis* are the most common causes, while in homosexuals *E. coli* is the main causative factor [26]. In 20% of the cases, the disease is nonspecific. Rare causes of the disease are brucellosis, tuberculosis, viruses, sarcoidosis, trauma or even drug administration such as amiodarone hydrochoride [6, 8, 14, 24, 28].

Gray scale ultrasonography demonstrates the hypoechoic appearance of the enlarged epididymis. In cases with testicular inflammation, the testis can also appear hypoechoic, enlarged and inhomogeneous [8, 24, 28]. Reactive hydrocele or scrotal wall thickening are present in most cases [22, 24, 26]. However, gray scale findings are nonspecific. Increased blood flow to the testis and epididymis, easily depicted by CDU, can correctly establish the diagnosis of inflammation. In 17 patients in our study, this was the only sign of the disease. Horstman et al., as well as other writers [22, 26, 28], report nine cases of epididymitis and eight cases of epididymo-orchitis with a normal appearance in gray scale US and increased vascularity in CDU. Clinical and laboratory findings can confirm the diagnosis. Dal Mo Yang et al. [17] report that the degree of blood flow was significantly greater in patients with non-specific epididymitis than in those with tuberculous epididymitis. In our series, the two cases of orcheoepididymitis that did not show increased vascularity were not caused by tuberculosis.

On MRI, the characteristic findings of epididymitis were enlargement, intermediate signal intensity on T2W images and intense enhancement of the epididymis and the spermatic cord. Increased signal intensity of the epididymis has been reported in other studies on both T1W and T2W images [43]. When the testis is involved, ill-defined areas of low signal intensity on T2W sequences were found. In one case with advanced disease, the testis involved had a high signal intensity on T2W images. Additional findings supporting the diagnosis could be the ill-defined border of the testis, the demonstration of normal or thickened testicular septations, the presence of reactive hydrocele, as well as thickening of the adjacent scrotal skin [5].

The most common complications include abscesses, pyocele or infarct [26]. A cystic fluid collection with irregular walls and increased peripheral ring-like vascular supply is a well established criterion for the diagnosis of an abscess [22, 26]. However, it is sometimes difficult to differentiate this image form that of a neoplasm. Follow-up after antibiotic administration and remission of the symptoms with improvement of the imaging findings make the diagnosis of neoplasm improbable [22], as we also observed in our study in three cases of abscess formation that were followed-up. In inconclusive cases, MRI has the potential to add valuable information on the distinction between inflammation and neoplasm [52].

Venous thrombosis in severe inflammation can lead to ischemia and infarct with similar imaging appear-

ances [22, 26]. Sanders et al. report that a reversal of flow during diastole in acute epididymo-orchitis is suggestive of venous infarction [42].

Fournier gangrene is a necrotizing fasciitis of the scrotum with a high mortality rate of about 75%, which is usually caused by *Klebsiella*, *Proteus*, *Streptococcus*, *Staphylococcus*, *Peptostreptococcus*, *E.coli* or *Clostridium perfrigrens* [7, 19, 47]. Gas is present in 18–62% of these cases and the characteristic appearance of multiple hyperechoic foci in the scrotum with the presence of reverberation artifacts in association with the clinical presentation can easily establish the diagnosis. A differential diagnosis of gas in the scrotum includes the presence of scrotal hernia. In the last case, the sonographer can depict the presence of air within the bowel and follow the course of the bowel within the peritoneal cavity.

A differential diagnosis between epididymitis and torsion is a diagnostic dilemma for the urologist. Both clinical manifestation and gray scale ultrasonography can be inconclusive. The fact that the pain cannot be relieved by elevating the scrotum, the absence of cremasteric reflex, the higher or transverse position of the testis are indicative of torsion. Gray scale ultrasonographic findings are not conclusive, as in torsion as well as in inflammation, the testis and epididymis can be enlarged, hypoechoic, and inhomogeneous with reactive hydrocele [8, 10, 24]. In the early stages of acute torsion, the testis may appear normal [8, 24, 26], while in rare cases it appears hypoechoic with hyperechoic mediastinum [8]. A complete absence of blood flow in the testis parenchyma is the main finding with CDU [8, 10, 26, 33], but normal extra-testicular flow can be detected [8]. In late torsions, increased blood flow in the scrotal wall can be present [26]. In cases of transient torsion, a mild increase in testicular and extra-testicular blood flow can be depicted and differential diagnosis of the torsion from orcheoepididymitis is impossible by means of US. In these cases, the acute onset of symptoms and the abrupt resolution can be indicative of transient torsion [26]. Decreased vascularity in comparison with the contralateral healthy testis can be the only imaging finding in cases of incomplete torsion [8, 26]. Suzer et al. report that physical examination and gray scale ultrasonography are insufficient for differentiating between inflammation and torsion in 45% of cases, while the diagnostic accuracy of CDU is 100% [45]. Burks et al. report a sensitivity of 86%, specificity of 100% and diagnostic accuracy of 97% for the demonstration of ischemia and torsion [10]. In our study, CDU has the high diagnostic accuracy of 93.5%.

In cases with acute torsion, the MR appearance of the testis remains normal and only in the subacute or chronic stage of the disease does the signal intensity of the testis change. In subacute cases, the testis appears enlarged with areas of high signal intensity on T1W images, indicating the presence of hemorrhagic elements. On the corresponding T2W images, the testis shows mixed signal intensity. In the chronic stage of the disease, the testis is usually small, and with a decreased signal on T2W images. Published data suggest that non-enhancement of the spermatic cord is the most sensitive and specific finding for torsion, and can help to differentiate between torsion and epididymitis [46]. The testicular salvage rate depends on the duration of ischemia. The salvage rate is 100% the first 6 h after the onset of symptoms, 70% after 6–12 h, and 20% after 12 h [8]. CDU being highly accurate and easy to perform, it is extremely valuable for the correct and quick diagnosis of torsion and saving of the testis.

Despite the fact that the testis is mobile in order to avoid trauma, direct force can lead to hematomas, contusions or rupture of the tunica albuginea. Ultrasonography can evaluate the extent of the traumatic lesion and the vascular supply to the testis. Scrotal wall hematomas are depicted as a thickening of the wall or fluid collection [26]. Blood collection between the tunica albuginea and tunica vaginalis represents hematocele, demonstrating varying echogenicity depending on the age of the trauma. Thrombus appears hyperechoic in the first days, becoming hypoechoic as the resolution progresses.

A large hematocele can displace the testis and obstruct the normal vascular supply resulting in atrophy of the parenchyma [26]. The evaluation of the integrity of the tunica albuginea is important. Rupture of the testis leads to orchectomy in more than 50% of the patients [26] if the surgery takes place in the first 72 h, while orchectomy is necessary in only 5–20% of the patients if the surgical restoration is immediate. In gray scale ultrasonography, testis rupture appears as an interruption of the tunica albuginea [24, 26]. Sometimes, however, it is difficult to evaluate the continuity of the echogenic line representing the tunica albuginea. On the other hand, hypoechoic areas in the parenchyma can represent hematomas or contusions without coexisting rupture of the tunica. Corrales et al. report that gray scale ultrasonography is invaluable in the investigation of trauma and propose surgical investigation [15]. On MRI, intra-testicular hematomas are demonstrated with high signal intensity on T1W images and mixed signal intensity on T2W images. The detection of tunica albuginea rupture could be an advantage of MRI when compared with US. Testicular trauma can sometimes mimic orcheoepididymitis (Fig. 4), neoplasm, pyocele or abscess [24]. Color Doppler ultrasonography can be helpful in the evaluation of these lesions, revealing hypervascularity in inflammation, variable vascularity in neoplasms and the absence of blood flow in hematoma [24, 33]. Suzer et al. report a diagnostic accuracy of 100% for CDU in traumatic scrotal lesions [45]

Clinical manifestation is usually indicative of the presence of a neoplasm. Most patients present with a painless palpable mass. In 10% of cases, neoplasms present acutely because of hemorrhage within the mass [24] or with hydrocele [29]. Only one of our patients presented with acute scrotum. Ultrasonography is unable to differentiate between benign and malignant

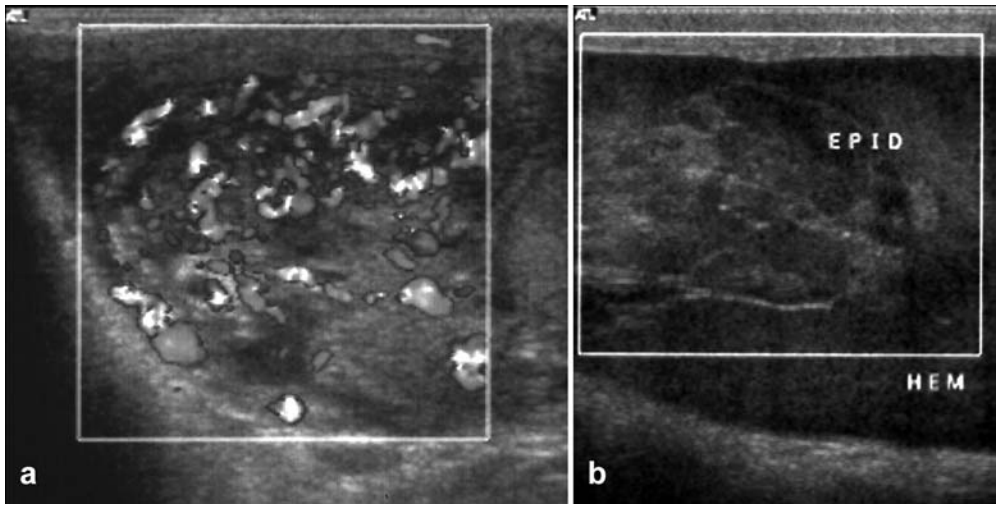

Fig. 4a,b Differential diagnosis between inflammation and trauma with the use of color Doppler ultrasound. Grey scale ultrasound shows similar findings, such as enlargement and inhomogenity of the epididymis in both cases. **a** Color Doppler ultrasonography depicts increased vascularity (epididymitis), **b** no flow was demonstrated (trauma)

lesions [20]. It can, however, differentiate between intra-testicular and extra-testicular masses [34]. Gray scale ultrasonography has a sensitivity of 100% for the detection of testis neoplasms. Carmignani et al. reported that there were, unfortunately, no clear parameters for differentiating between benign and malignant forms [11]. CDU can hardly offer additional information. According to Horstman et al. the tumor's vascular supply depends on its size and not on the histological type. Tumors smaller than 1.6 cm tend to be hypovascular, while tumors larger than 1.6 cm hypervascular [24, 29]. In our series, all neoplasms were larger than 1.5 cm and their vascularity varied greatly. Hypervascular neoplasms have a similar ultrasonographic appearance to inflammation using CDU [29]. Antibiotic administration and follow-up, as well as blood cancer tests, can help the differential diagnosis. Leukemic or lymphomatous infiltration of the testis can be bilateral and can present either as diffuse enlargement or as multiple hypo- or hyperechoic lesions [33]. In our cases with testicular tumors, T2W images proved to be absolutely accurate in revealing the mass (Fig. 5). However, a distinction between benign and malignant lesions, as well as the differentiation between different histological types of germ cell and stromal tumors by means of MRI was impossible. Both benign and malignant tumors have low signal intensity on T2W images with a variable degree of inhomogenicity. They are also both isointense to the testis showing a degree of enhancement [16, 35]. Previous reports claimed that seminomatous tumors could be more homogeneous than the non-seminomatous ones [43, 52]. MRI can also be used for local staging as well as for the detection of enlarged lymph nodes in the inguinal region and abdomen. A distinction between cysts and cystic tumors can be achieved by MRI with sensitivity reaching 100% [44, 52].

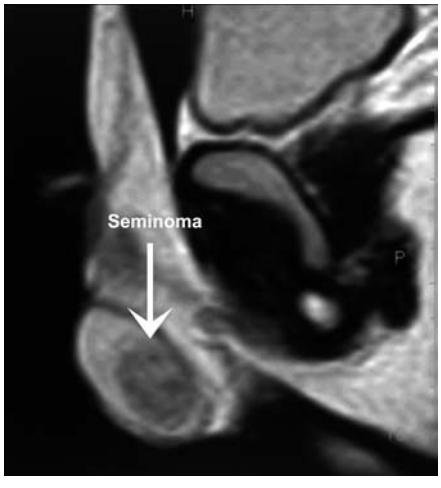

Fig. 5 Seminoma: sagittal T2W image. The seminoma is depicted as a well defined mass with inhomogeneous, low signal intensity, when compared to the testis

The association between testicular microlithiasis and cancer is a matter under discussion. Bach et al. report a high association of intra-testicular microlithiasis and confirmed testicular cancer [4]. Middleton et al. [36] report that the majority of patients with testicular tumors have coexistent microlithiasis, but also that 90% of the patients with microlithiasis did not have a tumor. In our study, microlithiasis was found in 13 patients, in four of whom a neoplasm coexisted. In one case, large calcifications in an atrophic testis led to FNA, which revealed the presence of adrenal rests in the testis (Fig. 6).

Ultrasonography is traditionally the method of choice for the detection of cystic lesions. In the scrotum, ultrasonography also allows the accurate diagnosis of cystic formations [12]. Loberant et al. report on how CDU could help the characterization of a cystic lesion by revealing flow within the septa of a complicated cyst that proved to be a cystic lymphangioma [31].

Tortuous anechoic structures in contact with the epididymis measuring more than 2 mm indicate the presence of varicocele with gray scale ultrasound. However, the presence of spermatocele cannot be ruled out. The depiction of flow within these structures, as well as the enlargement of the vessels in erect position or after Valsalva's maneuver confirm the presence of vari-

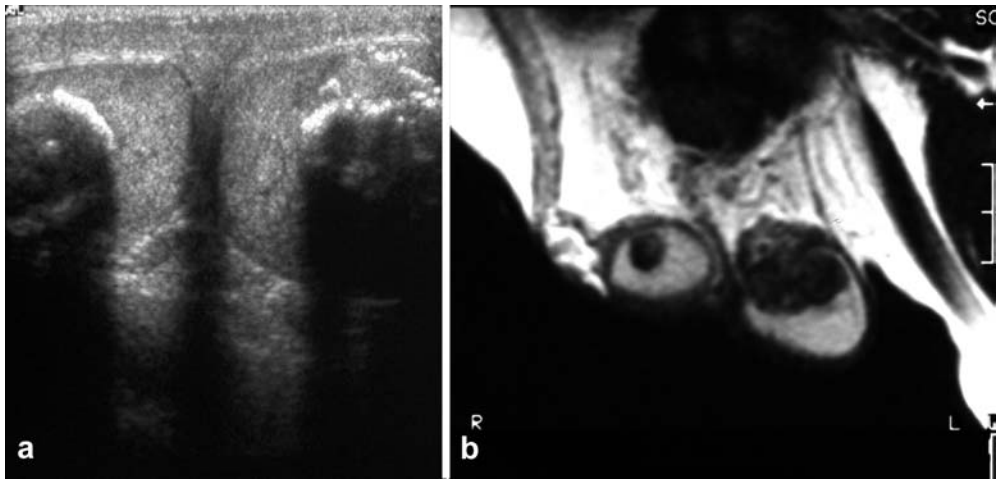

Fig. 6 Testis adrenal rests. **a** Gray scale depicts atrophy of both testes and multiple calcified round lesions. **b** On the corresponding MR image, the lesions are depicted with mixed low signal intensity on this T2W image

cocele [8, 24, 33]. Flow reversion in the veins during Valsalva's maneuver is compatible with valve insufficiency of the spermatic veins [39]. Petros et al. report that CDU can reveal subclinical varicocele responsible for infertility in a high percentage of cases. Blood flow cannot be depicted in cases of venous thrombosis [39]. Varicocele is more common on the left side. The left testicular vein, draining to the left renal vein, has to overcome a higher resistance than the right testicular vein emptying to the inferior vena cava. A reverse flow of blood results in varicocele more often on the left side [8].

The diagnosis of hydrocele is rarely a problem. Gray scale ultrasonography depicts an anechoic fluid collection in the scrotum. Internal echoes can sometimes be shown in the hydrocele due to the presence of inflammatory or hemorrhagic elements or the presence of cholesterol crystals [8].

The penis, as a superficial structure, is ideally suited for the ultrasonographic approach. US can access the extent of neoplasms and corpora invasion and can also determine whether a mass involves only the glans of the penis or the shaft as well. Horenblas et al. [27] report that US is not accurate enough for staging small tumors located at the glans. It can, however, reliably delineate the relationship of the tumor to the tunica albuginea, corpus cavernosa and urethra. Agrawal et al. report that in a series of 59 patients with penile carcinoma there was no significant association between echogenicity and tumor morphology or grade [1]. We agree to that both gray scale and CDU were not able to establish a specific pattern for echogenicity and blood flow between benign and malignant lesions. Lont et al. report a higher sensitivity for MRI than US or physical examination for the infiltration of the corpus cavernosum [32]. In our series, benign masses including fibroma and neuroma were located on the shaft outside of the corpora. Penile and urethral tumors may have an identical presentation on MRI. Both occur as inhomogeneous solid masses with a lower signal intensity on both T1W and T2W images compared to the corpora. They also have a variable degree of enhancement after contrast administration . Invasion of the tunica albuginea becomes obvious in MRI examinations and this is an advantage of the method for local tumor staging [40].

Peyronie's disease can manifest with focal or diffuse thickening of the tunica or with the formation of plaques that are usually calcified [13]. Calcification was depicted in all of our patients with Peyronie's disease. However, plaques may also present as hypoechoic or hyperechoic lesions, with increased vascularity when they are active. On MRI, the fibrous plaques when calcified are of low signal intensity and indistinguishable from the tunica albuginea. Active plaques demonstrate contrast enhancement (Fig. 7) and they can thus be easily identified.

Conclusions

Various studies [2, 3, 8, 10, 18, 22, 25, 26, 28, 29, 30, 33, 38, 39, 45, 49] report that CDU, which easily demon-

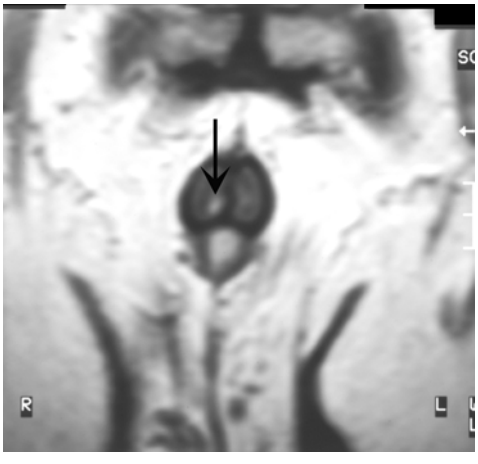

Fig. 7 Peyronie's disease: acute face. An axial T1W contrast enhanced image. The plaque is depicted as a bright lesion, due to the intense enhancement, a few millimeters wide within the right corpus cavernosa

strates vascular supply and blood flow, is a valuable tool in the diagnostic work-up of scrotal and penile diseases. According to our results, the CDU and power Doppler techniques are reliable in the diagnosis of orcheoepididymitis, estimating the extent of inflammation and revealing the presence of abscesses. CDU can also evaluate, with high diagnostic accuracy, the degree of blood flow in the testis or the absence of vascular supply in cases of trauma, being the main differential criterion between inflammation and torsion. Finally, it can easily depict the presence of varicocele and reveal subclinical cases. Ultrasonography is irreplaceable in the diagnosis of varicocele and torsion, and significantly improves the diagnostic accuracy in cases of inflammation or trauma.

Predicting the value of MRI in the evaluation of scrotum and penile diseases may be difficult, due to the relatively limited number of publications available. At present, MRI enables us to obtain high quality images of the normal anatomy and pathology of the testis, scrotum and penis. To our opinion, MRI will serve as a problem solving imaging modality, due to the high cost of the method and the high sensitivity and specificity of ultrasonography. Nevertheless, MRI can play an important role in the following: (1) the preoperative planning and local staging of testicular and penile tumors, (2) the detection of integrity of the tunica albuginea in trauma, and (3) the evaluation of cases for which ultrasound or clinical examination are inconclusive.

References

1. Al Multi RA, Ogedegbe AK, Lafferty K(1995) The use of Doppler ultrasound in clinical management of acute testicular pain. BJU 76:625–627
2. Atkinson GO, Patrick LE, Ball TI JR, Stepherson CA, Broecker BH, Woodard JR (1992) The normal and abnormal scrotum in children: evaluation with color Doppler sonography. AJR 158:613–617
3. Agrawal A, Pai D, Anantha Krishnan N, Smile SR, Ratnakar C (2000) Clinical and sonographic findings in carcinoma of the penis. J Clin Ultrasound 28:399–406
4. Bach AM, Hann LE, Hadar O, Shi W, You HH, Giess CS, Sheinfeld J, Thaler H (2001) Testicular microlithiasis: what is its association with testicular cancer? Radiology 220:70–75
5. Baker LL, Hajek PC, Burkhard TK, Dicapua L, Landa HM, Leopold GR, Hesselink JR, Mattrey RT (1987) Magnetic resonance imaging of the scrotum: pathologic conditions. Radiology 163:93–98
6. Bayram MM, Kervancioglu R(1997) Scrotal gray scale and color doppler sonographic findings in genitourinary brucellosis. J Clin Ultrasound 25:443–447
7. Benizri E, Fabiani R, Migliori G et al. (1996) Gangrene of the perineum. Urology 47:935–939
8. Bree RL, Hoang DT (1996). Scrotal ultrasound. Radiol Clin North Am 6:1183–1205
9. Brock G, Hsu GL, Nunes L (1997) The anatomy of the tunica albuginea in the normal penis and Peyronnie's disease. J Urol 157:276–281
10. Burks DD, Markey BJ, Burkhard TK, Balsara ZN, Haluszka MM, Canning DA (1990) Suspected testicular torsion and ischemia: evaluation with color Doppler sonography. Radiodogy 175:815–821
11. Carmignani L, Gadda F, Gazzano G, Nerva F, Mancini M, Ferruti M, Bulfamante G, Bosari S et al. (2003) High incidence of benign testicular neoplasms diagnosed by ultrasound. J Urol 170:1783–1786
12. Cook LJ, Dewbury K (2000) The changes seen on high-resolution ultrasound in orchitis. Clin Radiol 55:13–18
13. Corrales JG, Corbel L, Cipolla B et al. (1993) Accuracy of ultrasound diagnosis after blunt testicular trauma. J Urol 150:1834–1836
14. Cho JH, Chang JC, Park BH, Lee JG, Son CH (2002). Sonographic and MR imaging findings of testicular epidermoid cysts. AJR 178:743
15. Chou YH, Tiu CM, Pan HB et al. (1987). High resolution real time ultrasonography in Peyronie's disease. J Ultrasound Med 6:67–70
16. Cramer B, Schlegel E, Thuerolf J (1991) MRI in the differential diagnosis of scrotal and testicular disease. Radiographics 11:9-21
17. Dal Mo Yang DM, Kim SH, Kim HN, Kang JH, Seo TS, Hwang HY, Kim HS, Cho H (2002) Differential diagnosis of local epididymal lesions with gray scale. Sonographic, color Doppler sonographic and clinical features. J Ultrasound Med 22:135–142
18. Dewier DM, Begun FP, Lawson RK, Fitzgerald S, Folley WD (1992) Color doppler ultrasonography in the evaluation of the acute scrotum. J Urol 147:89–91
19. Dogra VS, Gottlied RH, Oka M, Rubens DJ (2003) Sonography of the scrotum. Radiology 227:18–36
20. Dogra VS, Gottlied RH, Rubens DJ, Liao L (2001). Benign intratesticular cystic lesions: US features. Radiographics 21:5273
21. Doubilet PM, Benson CB, Silverman SG, Gluck CD (1991) The penis. Semin Ultrasound CT MR 12:157–175
22. Ferriol VG, Cornelia XP, Agrornayor EG, Greixarns XS, Martinez de la Torre JB (2000) Gray scale and power Doppler sonographic appearances of acute inflammatory diseases of the scrotum. J Clin Ultrasound 28:67–72
23. Gabella G (1995) Cardiovascular. In: Williams PL, Bannisher LH, Berry MM et al. (eds) Gray's anatomy. Churchill Livingstone, New York, pp 1451–1626
24. Gersovich EO (1998) Scrotum and testes. In: McGahan JP, Goldvberg BB (eds). Diagnostic ultrasound. A logical approach. Lipincort-Raven, Philadelphia, pp 893–933
25. Hawtrey CE (1998) Assessment of acute scrotal symptoms and findings. A clinicians dilemma. Urolic Clin North Am 4:715–723
26. Herbener TE (1996) Ultrasound in the assessment of the acute scrotum. J Clin Ultrasound 24:405–421
27. Horstman WG, Middleton WD, Melson GI (1991) Scrotal inflammatory disease: color Doppler US findings. Radiology 179:55–59
28. Horstman WG, Melson GL, Middleton WD, Andriole GL (1992) Testicular tumors: findings with color Doppler US. Radiology 185:733–737
29. Horenblas S, Kroger R, Galee MP, Newling DW, Van Tinteren H (1994) Ultrasound in squamous cell carcinoma of the penis; a useful addition to clinical staging? A comparison of ultrasound with histopathology. Urology 43:702–707
30. Krieger LN, Wang K, Mack L (1990). Preliminary evaluation of color Doppler imaging for investigfation of intrascrotal pathology. J Urol 144:904–907
31. Loberant N, Chernihorski A, Godfeld M, Sweed V, Vais M, Tzilman B, Cohen I (2002) Role of Doppler sonography in the diagnosis of cystic lymphangioma of the scrotum. J Clin Ultrasound 30 :384–387
32. Lont AP, Besnard AP, Galee MR, Van Tinteren, Horenblas S (2003) A comparison of physical examination and imaging in determining the extent of primary penile carcinoma. BJU 91 :493–495
33. Luker GD, Siegel MJ (1994) Color Doppler sonography of the scrotum in children. AJR 163:649–655
34. Michallef M, Torreggiani WC, Hurley M, Dinsmore WW, Hogan B(2000) The ultrasound investigation of scrotal swelling. Int J STD AIDS 11:297.

35. Muller-Leisse C, Bohudrf K, Stargardt A, Sohu M, Adam G (1994) Gadolinium-enhanced T1 W versus T2 W imaging of scrotal disorders: is there an indication for MR imaging? JMRI 4:389–395
36. Middleton WD, Thorne DA, Melson GL (1989) Color Doppler ultrasound of the normal testis. AJR 152:293–297
37. Middleton WD, Teefey SA, Santillan CS(2002) Testicular microlithiasis: prospective analysis of prevalence and associated tumor. Radiology 224 :425–428
38. Patriquin HB, Yazbeck S, Trinh B et al. (1993) Testicular torsin in infants and children: diagnosis with doppler sonography. Radiology 188:781–785
39. Petros JA, Andriole GL, Middleton WD, Dicus DA (1991) Correlation of testicular color Doppler ultrasonography, physical examination and venography in the detection of left varicoceles in men with infertility. J Urol 145:785–788
40. Pretorous S, Siegelman E, Ranchandami P, Banner M (2001) MR imaging of the penis. Radiographics 21:283–298
41. Rubin JM, Bude RO, Carson PL, Bree RL, Adier RS (1994) Power Doppler US: a potentially useful alternative to mean-frequency lased color Doppler US. Radiology 190:853–856
42. Sanders LM, Haber S, Dembner A, Aquino A (1994) Significance of reversal of diastolic flow in the acute scrotum. J Ultrasound Med 13:137–139
43. Sica G, Teeger S (1996) MR imaging of scrotal, testicular and penile diseases: MRI clinics of North Am. Vol 4:545–563
44. Stikkelbroeck N, Suliman H, Otten B, Hermus A, Blickmay J, Jager G (2003) Testicular adrenal rest tumors in postpubertal males with congenital adrenal hyperplasia sonographic and MR features. Eur Radiol 13:1597–1603
45. Suzer O, Oacan H, Kupeli S, Gheiler EL (1997). Color Doppler imaging in the diagnosis of acute scrotum. Eur Radiol 32:457–461
46. Trambert MA, Mattrey RF, Levine D, Berthoty DP (1990) Subacute scrotal pain: evaluation of torsion versus epididymitis with MRI. Radiology 175:53–56
47. Vick R, Carson CC(1999) Fournier's disease. Urol Clin North Am 26:841–849
48. Watanabe Y, Dohke M, Okkubok K, Ishimori T, Amoh Y, Okumura A, Odd K, Hayashi T, Arai V (2000) Scrotal disorder : evaluation if testicular enhancement patterns at dynamic contrast subtraction MR imaging. Radiology 217:219–227
49. Wilbert DM, Schaerfe CW, Stern WD, Strohmaier WL, Bichler KH (1993) Evaluation of the acute scrotum by color coded doppler ultrasonography. J Urol 149:1475–1477
50. Williams PL (1989). Splachnology. In: Williams PL, Warwick R, Dyson M, Bannister LH (eds) Gray's anatomy. Churchill Livingstone, London, pp 1432–1433
51. Wilkins CJ, Sriprasas S, Sidhu PS (2003) Color Doppler ultrasound of the penis. Clin Radiol 58 :514–523
52. Woodward P, Sohaey R, O'Donoghue M, Green D (2002) Tumors and tumor-like lesions of the testis: radiologic-pathologic correlation. Radiografics 22:189–216